IRAQI Academic Scientific Journals
Samarra Journal of Pure and Applied Science
SJPAS
www.sjpas.com
p ISSN: 2663-7405
e ISSN: 2789-6838

Synthesis, characterization, Liquid crystal properties study, molecular docking simulation and antibacterial activity of new porphyrin esters

Satar Jubair Mayof *, Hanaa Kaain Salih
Department of Chemistry, College of Science, Tikrit University, Iraq

https://doi.org/10.54153/sjpas.2025.v7i4.1143

Article Information
Received: 19/02/2025
Revised: 20/03/2025
Accepted: 20/03/2025
Published: 30/12/2025

Keywords:
Liquid crystal, Molecular docking, Porphyrin ester, Antibacterial activity

Corresponding Author
E-mail: satar.jubair@st.tu.edu.iq
Mobile: 07826409385

Abstract

This report highlights preparing a new porphyrine ester molecule. the first step initially, synthesis of core structure (porphyrine) through condensing of pyrrole with p-hydroxybenzaldehyde in propionic acid. Then 4-hydroxy ethyl benzoate (S9) was prepared then linked to porphyrin core structure to constitute S10 derivative. Finally, S10 derivative esterified with various carboxylic acids to obtain (S11-S17) compounds. The structure of ultimate compounds was established by FT-IR, ^{1}H-NMR and ^{13}C-NMR, where the obtained results confirmed the suggested structure. The liquid crystal feature of these molecules was established via polarized light microscope equipped with a heater (POM) where the obtained derivatives (S12-S15) showed distinct liquid crystal phases. Molecular docking investigation was performed for the high antibacterial obtained derivatives (S11-S13) where the results showed these derivatives with a good docking score and best binding images.

Introduction

Historically, since the important discovery of the homogeneous porphyrin called porphycin by E. Vogel [1] which revolutionized porphyrinoid chemistry, a wide range of porphyrins and their derivatives have become available to researchers[2]. Calxipyrroles, contracted porphyrinoids, extended porphyrinoids, heteroatom-exchanged porphyrinoids, and inverted porphyrinoids are examples that can be cited[3]. The formation of highly conjugated derivatives has been achieved by elongating the system using polycyclic aromatic rings fused to the periphery of the macrocyclic core[4]. A new family of fully synthetic tetrapyrrole macrocycles known as phthalocyanines and their derivatives [5].

Porphyrins play an important role in biological systems. They are involved in the conversion of light to chemical energy (photosynthesis), in electron transfer processes or in the transport of oxygen (respiration)[6, 7]. The particular chemical structure of the porphyrins with a circular π-electron system gives rise to unusual photo-physical properties of single molecules as well as to molecular association phenomena causing efficient energy delocalization [8].

According to reports, porphyrins have a wide range of biological actions[9]. Since free radical-mediated peroxidation of membrane lipids and oxidative damage of DNA were thought to be linked to a number of chronic health issues, including cancer[10], atherosclerosis[11], neurodegenerative diseases[12], With aging, it was also believed that porphyrins' antioxidant properties were linked to their desirable cancer-prevention or potential therapeutic benefits [13]. According to reports, the majority of synthetic and natural porphyrins are ineffective against Gram (-) bacteria. However, new forms of water-soluble cationic porphyrins that have hydroxyethyl, butyl, or allyl functional groups replaced in the meso position [14].

Materials and Methods

All chemicals were imported from Sigma Aldrich. Melting points were measured for synthesized compounds by Gallen-Kamp MFB-600 apparatus. The FT-IR spectra were established on an FT-IR-8400S-Shimadzu spectrophotometer. Mass spectra were performed by Shimadzu model GCMSQP 1000 EX spectrometer (Japan). NMR spectra were recorded on VARIAN-INOVA 500 MHZ spectrophotometer (Germany), deuterated solvent (DMSO-d6) was used, and tetramethylsilane TMS was used as an internal standard The liquid crystal phases studied and characterized by polarized light microscope equipped with a heater (POM.)

Preparation of tetrakis(4-hydroxyphenyl)porphyrin (THPP)center core[15]**:**

In a three-hole round-bottomed flask with a capacity of (IL) equipped with a reflective condenser (0.1025mo1), (12.5g) para-hydroxybenzaldehyde dissolved in (750ml) Propionic acid was placed, then (7.1ml) (0.1025mol) pyrrole was added to the flask gradually with continuous stirring. The mixture left to reflux for 30 minutes. Then the reaction mixture was cooled to room temperature, and a purple precipitate was formed. The precipitate was filtered using a Buchner funnel (under vacuum), then the precipitate was washed with a small amount of ethanol and then with distilled water. The precipitate was dried using an electric oven at a temperature of (70-50) °C for 30 minutes to produce (4g) at a ratio of (23%) and it was recrystallized from ethanol. The resulting compound was dark purple color with m.p = > 300. As shown in the following Scheme (1).

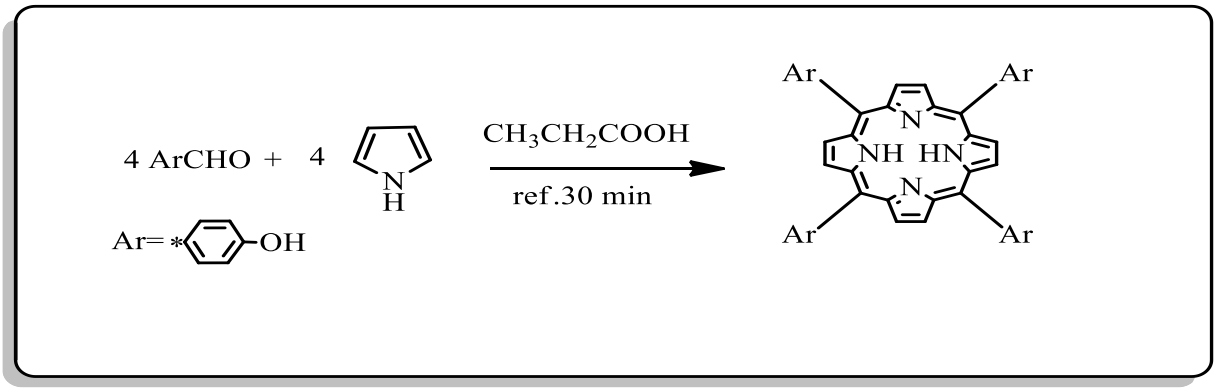

Scheme 1: preparation of tetrakis (4-hydroxyphenyl) porphyrin (THPP).

Preparation of acidified ethanol[16]**:**

In a round-bottomed flask with a capacity of (100 ml) 30 g of NaCl introduced to this round, then, many drops of sulfuric acid added, HCl gas liberated through tube into reception beaker containing of absolute ethanol, the bubbles observed until the alcohol saturated by HCl gas as shown in scheme (2).

Synthesis of ester compound S9[16]**:**

In a round-bottomed flask with a capacity of (100 ml) 30 mL of acidified ethanol was mixed with 5g of Para-hydroxy benzoic acid, then the mixture was refluxed for 6hrs, then cooled, stirred for 1h, the precipitate was formed, collected, dried and treated by sodium bicarbonate solution recrystallized by absolute ethanol. yield= 92%, m.p=117 ^{o}C. As shown in the following Scheme (2).

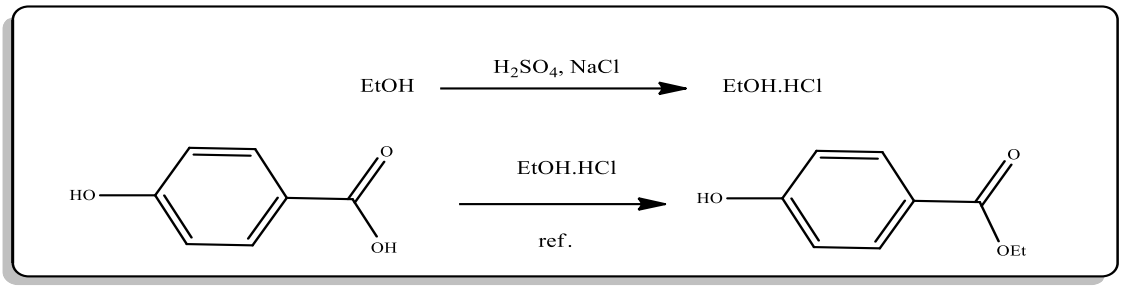

Scheme 2: preparation of ester S9.

Synthesis of ester compound S10[17]**:**

In a 50 mL round-bottom flask containing 20 mL of absolute ethanol, 0.004 mol (2.75g) of tetrakis(4-hydroxyphenyl) porphyrin (THPP)is dissolved to this (0.016 mol,2.64g) of prepared ethyl 4-hydroxy benzoate dissolved in absolute ethanol is added. After the addition is complete, the reaction mixture is refluxed for 6 hours. The progress of the reactions was monitored using thin-layer chromatography (TLC) and iodine staining. Upon completion of the reflux period, the mixture was cooled and stirred for an additional hour. precipitate formed formed was noticed, collected, dried, and recrystallized using ethanol, yield= 88%, m.p=277 ^{o}C. As shown in the reaction equation (3).

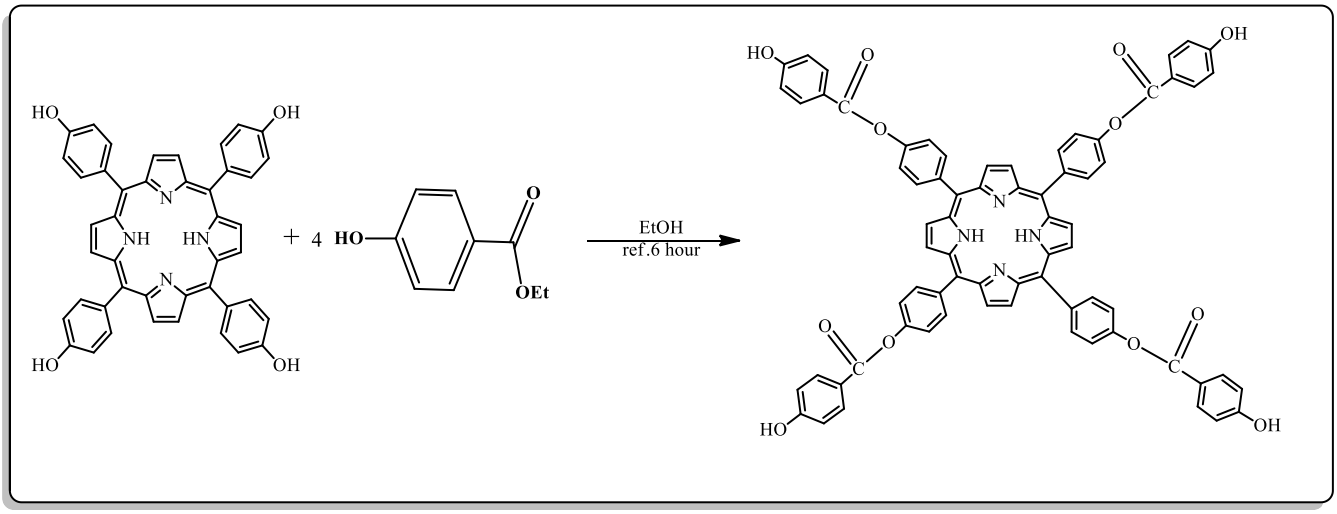

Scheme 3: preparationof **ester** S10.

Synthesis of esters compounds S11-17[18]:

To a 50 mL round-bottomed flask immersed in an ice bath and containing 20 mL of pyridine and compound (S10) (0.4g, 0.00059 mol), one of acid chlorides (0.0024 mol) was added. The mixture was stirred at room temperature for 24 hours. Thereafter, the mixture was poured into a beaker containing crushed ice, acidified with 10% HCl, and the solid product was filtered, washed with water, and recrystallized from benzene. TLC was

performed using acetone-hexane (3:7) as the eluent solution. Table 1 shows some of the physical properties for the prepared compounds (**S11-S17**), as shown in the Scheme (4):

Table 1: Physical characters of synthesized compounds (**S11-S17**).

Comp. Symb.	Molecular Formula	Mol.Wt. gm/mole	Yield %	R_f *Eluent 7hexane 3Acetone*	Color	m.p ^{0}C
S11	$C_{80}H_{54}N_4O_{16}$	1326.30	79	0.62	Dark Brown	277-279
S12	$C_{84}H_{62}N_4O_{16}$	1382.41	76	0.81	Dark Brown	280-282
S13	$C_{88}H_{70}N_4O_{16}$	1438.51	74	0.76	Dark Brown	274-276
S14	$C_{92}H_{78}N_4O_{16}$	1494.62	81	0.72	Dark Brown	271-273
S15	$C_{96}H_{86}N_4O_{16}$	1550.73	73	0.74	Dark Brown	269-171
S16	$C_{100}H_{94}N_4O_{16}$	1606.83	69	0.67	Dark Brown	270-272
S17	$C_{112}H_{118}N_4O_{16}$	1774.15	72	0.71	Dark Brown	278-280

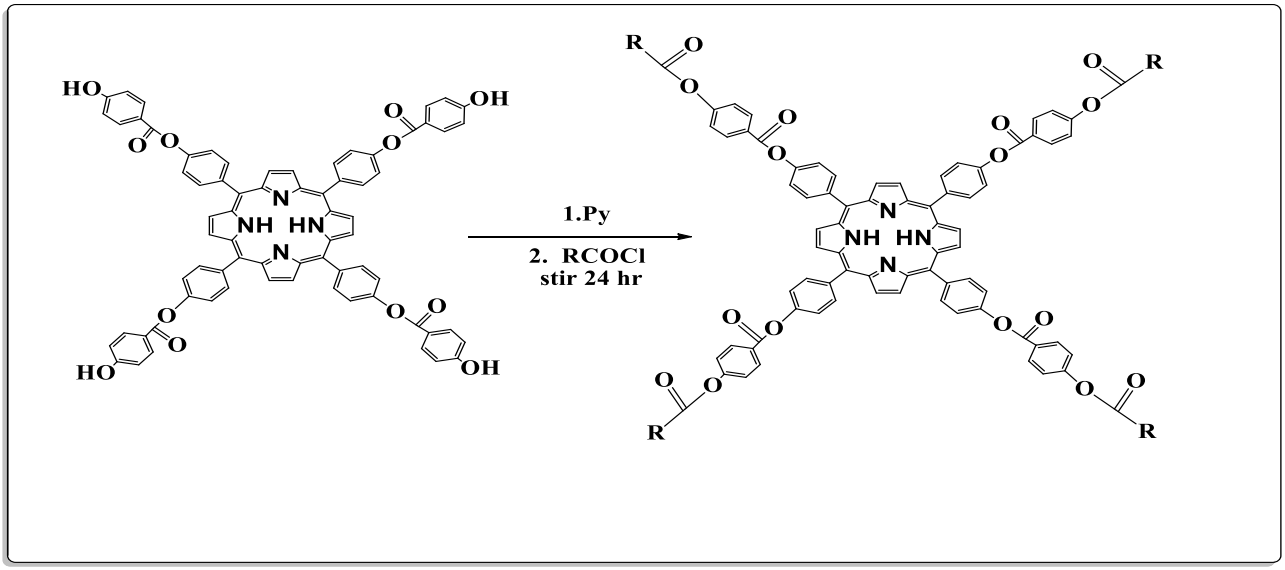

Scheme 4: **Preparation of esters S11-S17.**

Antibacterial activity estimation protocol[19]**:**

The antibacterial efficacy of the novel porphyrin derivatives were investigated against, *Escherichia coli* and *Staphylococcus aureus*, pathogenic bacteria as the following*:*

Culture media: Mueller-Hinton agar used as culture media and prepared by dissolving 38g of material in 1000 mL of distilled water, then immersed and heated with stirring to obtain a

clear solution. Sterilized via autoclave, cooled to 47 ^{o}C and introduced a petri-dish at sterilized conditions.

Inoculation of culture media: Culture media was inoculated by inoculum bacterial suspension (1.5 x 10^{8} CFU/mL), inoculation process was accomplished via a cotton swab in three directions, the plate left for 15-20 min until drying of the media.

Sensitivity assay: Estimation of efficacy of new porphyrin derivatives versus to pathogenic types of bacteria was investigated by well diffusion method then incubated at 37 ^{o}C. The inhibition of culture was measured after one day and with reference drugs, Amikasine.

Molecular docking protocol[20]**.**

This study includes molecular modeling study; this term indicates designing the candidate lead compound by computer software. Molecular docking studies were investigated via employing Auto Dock vina programs. biotin carboxylase (**PDB:ID: 3jzf**), biotin protein ligase **(PDB:ID:4dq2**) were downloaded from RCSB, PDB (Protein Data Bank) site. In regarding enzyme, water molecules were removed and polar hydrogens were added as well as kolman charge this process were performed by Auto Dock tool 1.5.6 program. The visualization binding mods of ligand were performed by Discovery Studio 2020 Client**.**

Results and Discussion:

The center core tetrakis(4-hydroxyphenyl) porphyrin (THPP) was synthesized through condensed of p-hydroxy benzaldehyde with pyrrole in the medium of propionic acid, then the THPP reacted with 4-hydroxy ethyl benzoate (**S9**) to generate **S10** compounds. Finally, S10 molecule esterified with various carboxylic acids to obtain the (**S11-S17**) compounds as explained in the following scheme (5).

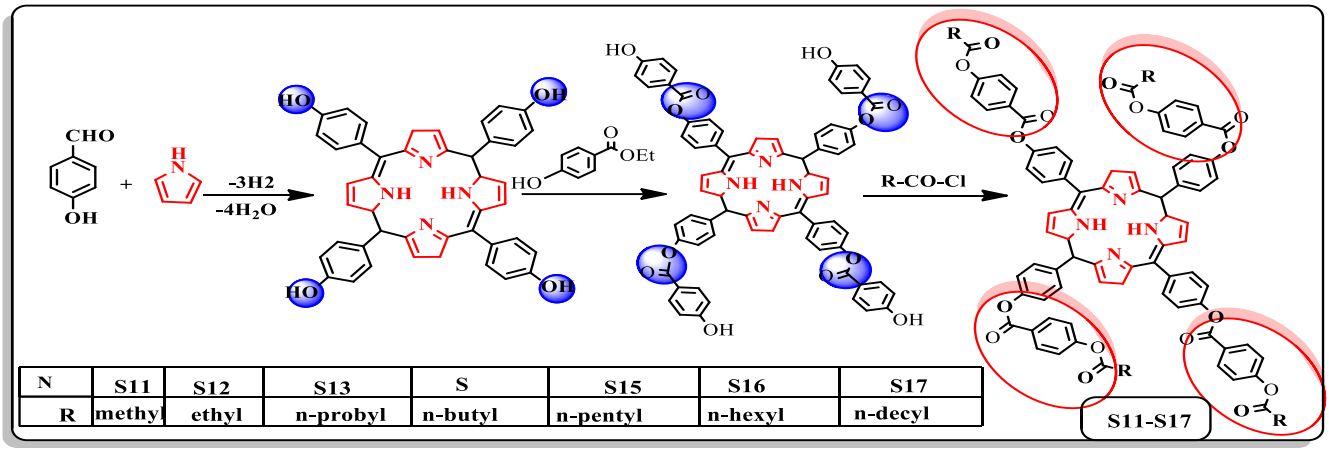

N	S11	S12	S13	S	S15	S16	S17
R	methyl	ethyl	n-probyl	n-butyl	n-pentyl	n-hexyl	n-decyl

Scheme (5): Synthetic path of new porphyrin esters.

The spectral techniques used to establish the proposed structure as follow:

The FT-IR spectrum of THPP compound (Figure 1) revealed the following: the band at 3412 cm^{-1} return to O-H group, the band at 3234 cm^{-1}, represent (N-H) group of pyrrole, the (C-N) group vibrated at 966 cm-1, the C-H aromatic observed at 3014 cm^{-1}, the (C=C) aromatic vibrated at wave number1508 –1606 cm^{-1} while the(C=N) observed at (1232-1367) cm^{-1}.[21].

^{1}H-NMR: of THPP compound(Figure 2) revealed: singlet signal at the chemical shift -2.27 ppm (s , 2H , NH) corresponding to amine group of pyrrole in center core of THPP compound , the peaks at δ= 6.34 – 6.99 ppm return to aromatic protons, singlet signal at δ= 6.95 ppm refer to proton of O-H in phenol moiety , the doublet signal at δ= 8.32 ppm, (dd, 8H, β-pyrrole) represent o alkenic protons.

^{13}C-NMR of THPP compound (Figure 3) showed the following data: the signal at δ= 158.18 ppm, attributed to C-O of phenol, the signals at range δ= 117.29 – 133.2 ppm, refer to aromatic carbons. The signal at δ= 147.73 ppm corresponds to (C=N) group in pyrrole section, the signal at δ= 137.8 ppm refer to (C-NH-C-) in pyrrole rings[22].

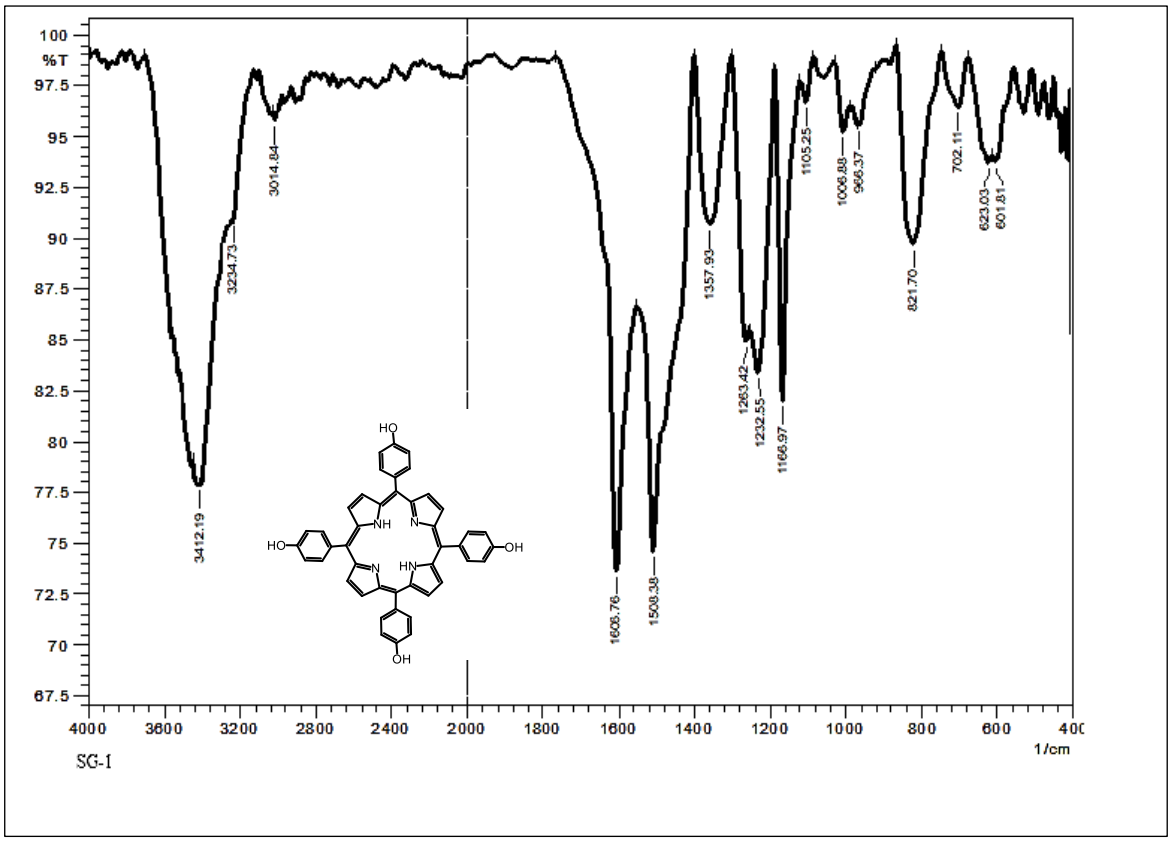

Fig. 1 FT-IR spectrum of porphyrin THPP compound.

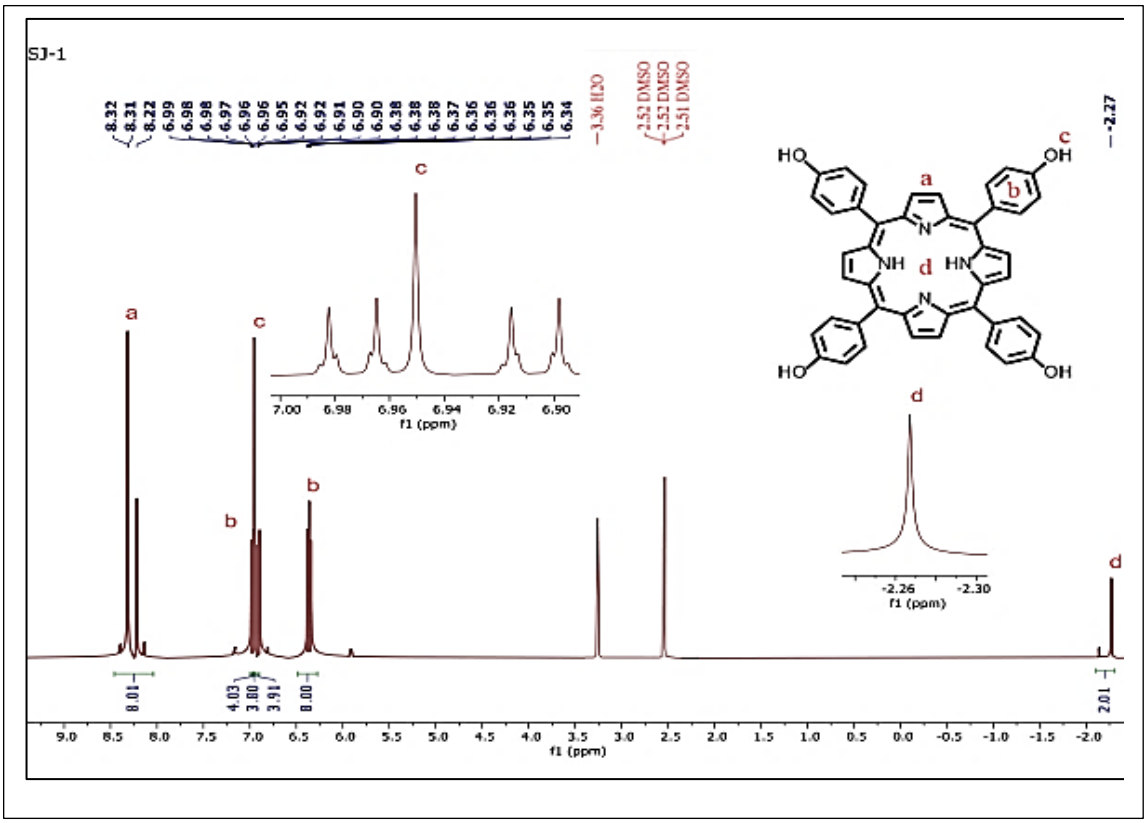

Fig. 2 ^{1}H-NMR spectrum of porphyrin THPP compound.

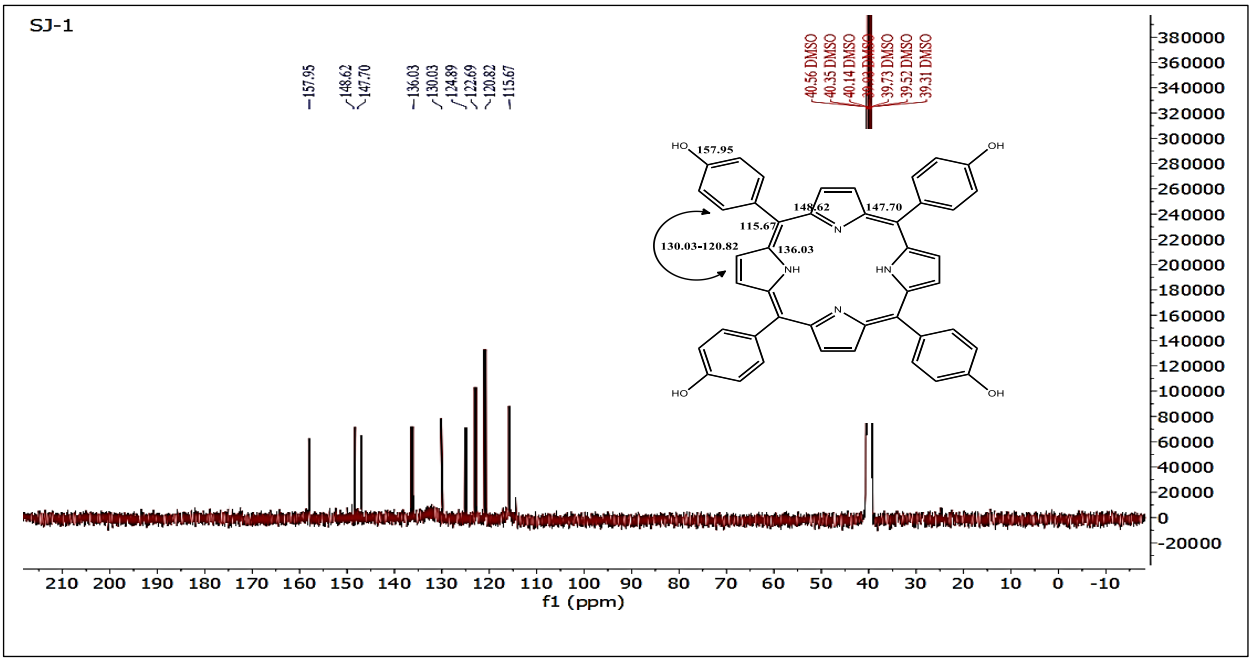

Fig. 3 ^{13}C-NMR spectrum of porphyrin THPP compound.

Characterization of S9 derivative

The prepared compound ethyl 4-hydroxybenzoate (S9) was characterized by melting point and color. The IR spectrum of the compound (S9) Figure 4 showed an absorption band at frequency (3227 cm^{-1}) due to the stretching of the υ(O-H) bond, and two absorption bands were observed in the range (2975-2888 cm^{-1}) attributed to the symmetric and asymmetric

stretching vibration of the aliphatic υ(C-H) bond. In addition, the absorption band at frequency (3064 cm^{-1}) due to the stretching vibration of the aromatic υ(C-H) bond, while the carbonyl group of the ester υ(C=O) appeared in the range (1747 cm^{-1}), which confirms the formation of the ester. The absorption band at the frequency (1608-1519 cm^{-1}) is attributed to the stretching vibration of the υ(C=C) bond, while the absorption band at the frequency (1168 cm-1) is attributed to the stretching vibration of the υ(C-O) bond[23]..

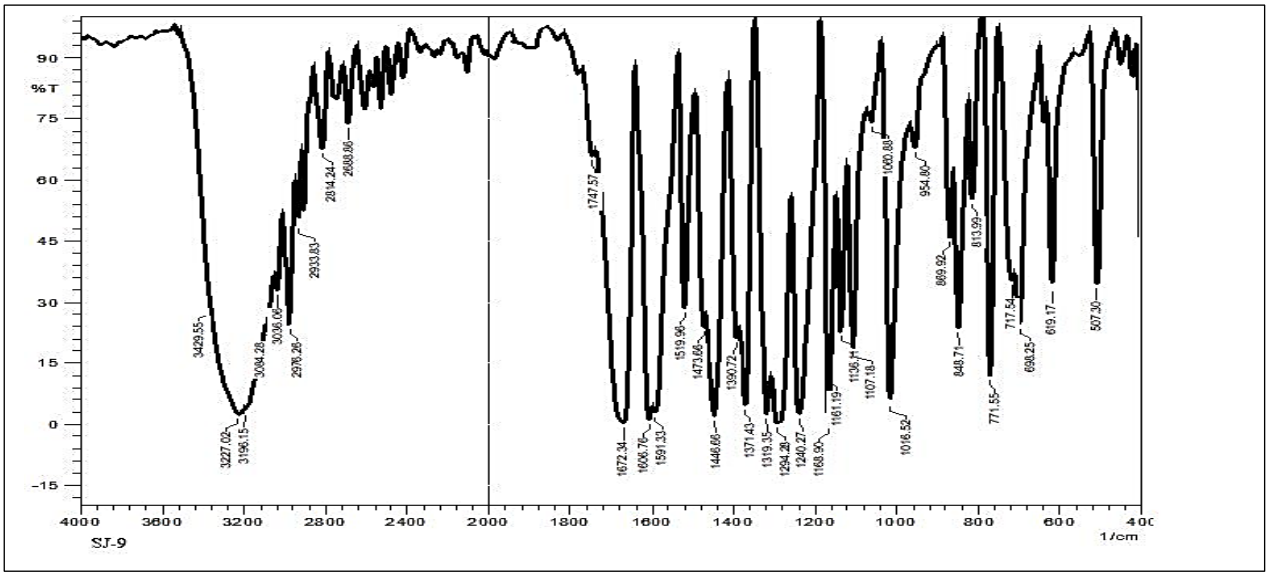

Fig. 4 FT-IR spectrum of **S9** compound.

Characterization of S10 derivative:

The structure of S10 compound was confirmed by FT-IR (Figure 5) as follow: the peak at 3500- 2800 cm-1 refer to(O-H) of carboxylic group , the peak at wave number 1730 cm^{-1} represent of carbonyl group, the N-H of pyrrole in center core observed at range 3217 cm^{-1}, the C-H aromatic observed at range 3084cm^{-1} , the C=C observed at range 1606 cm^{-1} , the C-N of pyrrole ring vibrated at range 1369 cm^{-1} [21].

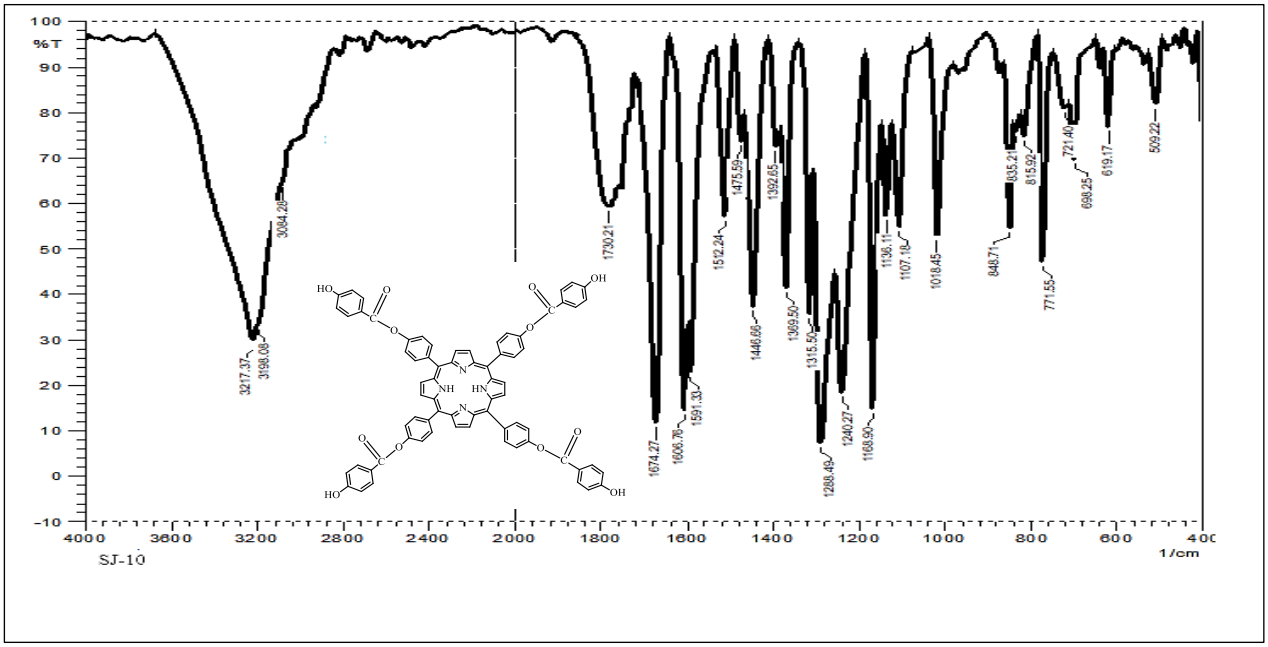

Fig. 5 FT-IR spectrum of **S10** compound.

Characterization of porphyrine derivative (S11-17):

The FT-IR spectra for compounds **S11-S17** (see Figure 6,7 for a representative case of **S11,S17**) showed absence the peak at 2800 -3500 that indicated to ν(O-H) of carboxyl group, the wave number of C=O appeared at 1710-1763 cm-1, the C-H aliphatic was vibrated at range 2926 – 2982 cm-1, the C-H aromatic was emerged at 3068 – 3078 cm-1, N-H group vibrated at frequency 3219 – 3273 cm^{-1}, the C-N of pyrrole appeared at 1350 – 1357 cm-1, C=C aromatic vibrated at 1508 – 1606 cm^{-1} [21]in the table 2.

Table 2: FT-IR spectrum data of porphyrine derivative **(S11-17)**.

Comp	νC-H		νC=O	νN-H	νC=C	νC=N	νC-N Arom	νC-O	νO-H
	Arom	Aliph.	Ester						
S11	3070	2982	1763	3250	1602	1502	1356	1203-1165	–
S12	3068	2982	1761	3244	1602	1504	1357	1274-1163	–
S13	3070	2966	1757	3273	1602	1502	923	1276-1163	–
S14	3078	2960	1761	3250	1602	1504	1369	1276-1163	–
S15	3074	2958	1755	3238	1604	1506	1375	1276-1163	–
S16	3070	2929	1761	3248	1602	1506	1373	1276-1163	–
S17	3070	2926	1710	3219	1602	1512	1389	1280-1166	–

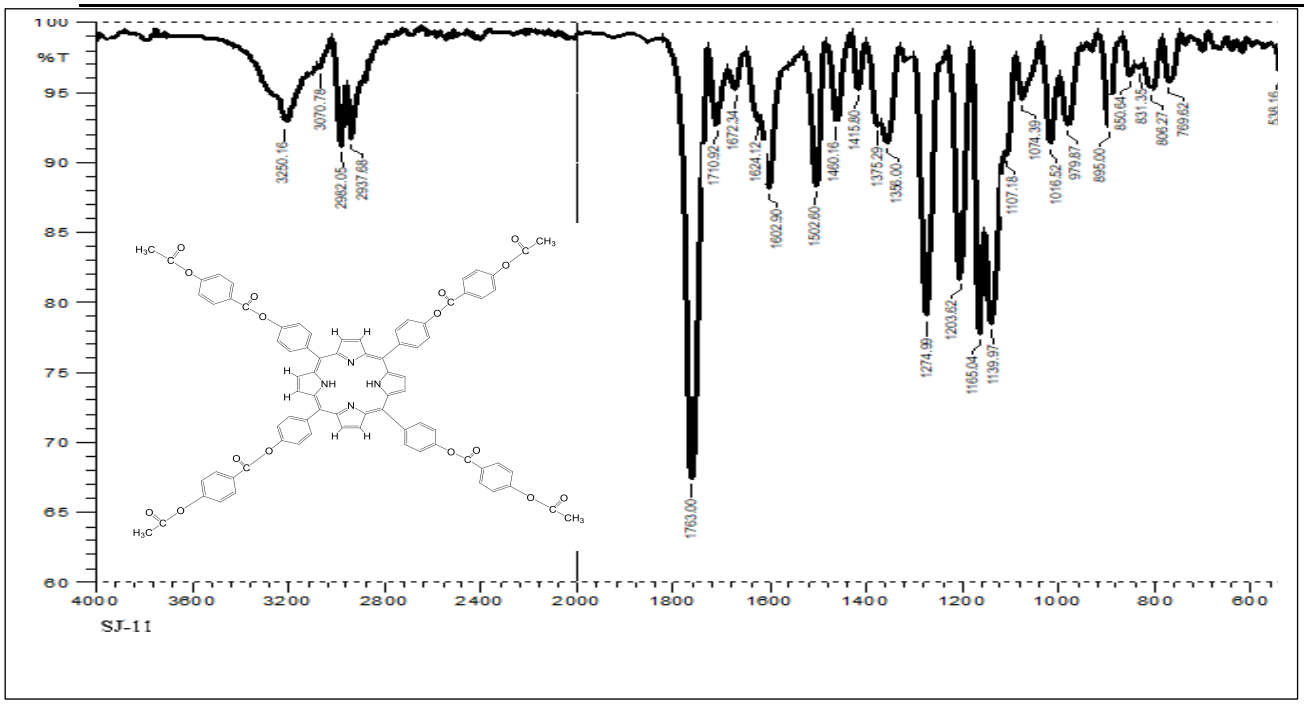

Fig. 6 FT-IR spectrum of **S11** compound.

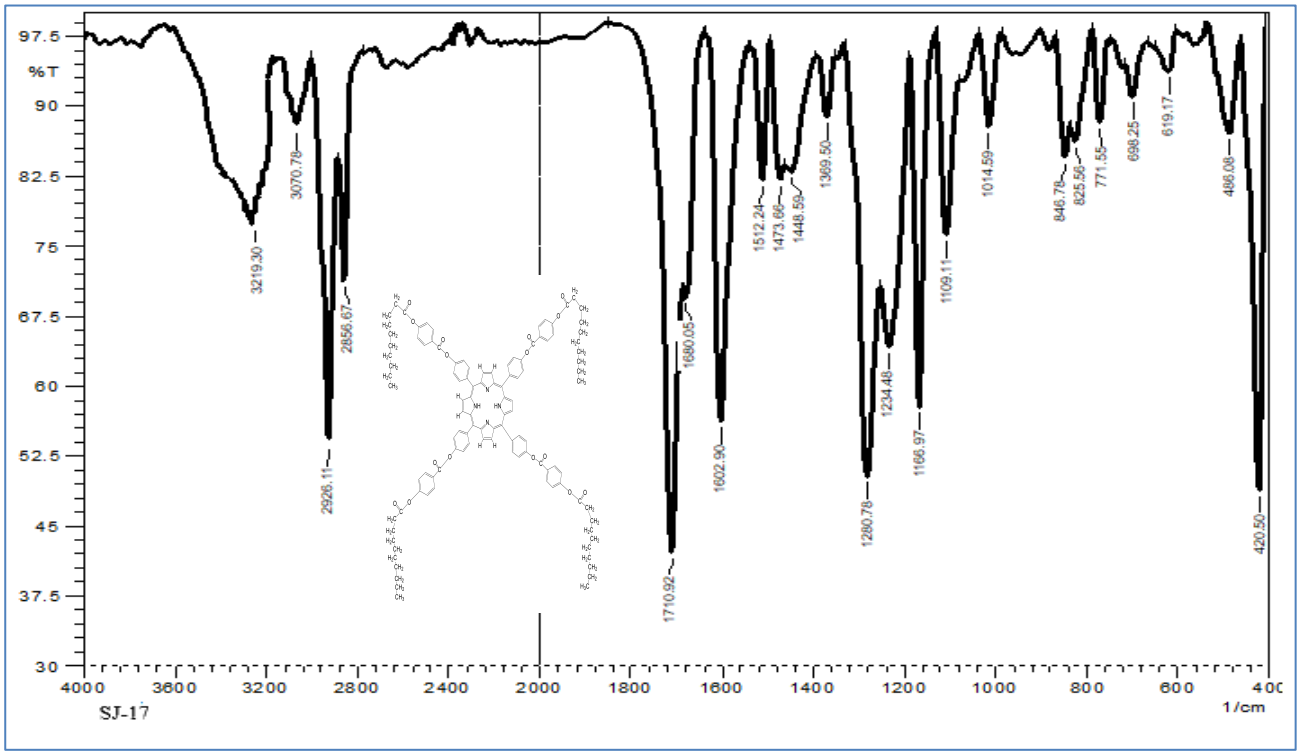

Fig. 7 FT-IR spectrum of **S17** compound.

According to ^{1}H-NMR spectra for compounds **S11-17**, the OH signal at 6.95ppm attributable to compound **THPP** has disapeared, aromatic proton signals were observed within the range δ 6.52–7.52 ppm, while proton signals for alkyl groups were observed within the range δ 0.28-2.07 ppm. and table 3. Chemical Shift δ ppm of **(S11-17)** [22]**.**

The ^{1}H-NMR spectrum of **S11** figure 8. Revealed singlet signal at =-2.27 ppm represent the protons of NH groups in pyrrole moiety. doublet signal at range 6.62- 7.52 ppm refer to the aromatic protons, singlet signal at 1.78 ppm refer to the CH_3 protons. Doublet signal at =8.32 ppm refer to the alkenic protons of at beta position in pyrrole(-C=C<u>H</u> Pyrrole).

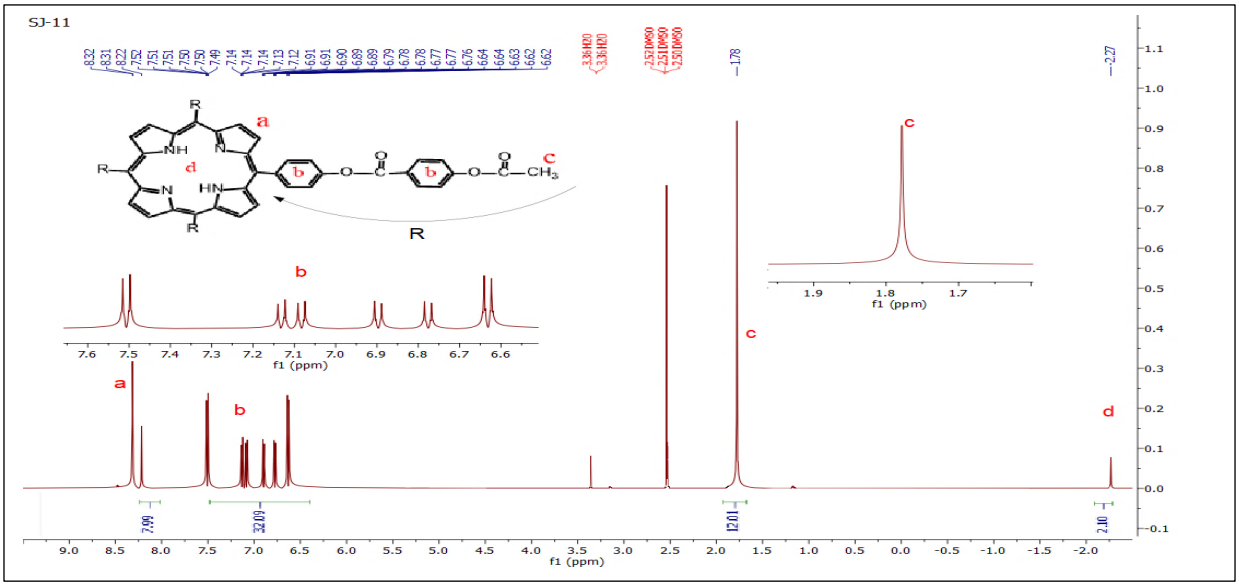

Fig. 8 FT-IR and ^{1}H-NMR spectrum of **S11** compound.

^{1}H-NMR spectrum of **S13** figure 9. Revealed the following. Chemical shift at = - 2.27ppm (s, 2H,NH) corresponding to the amine groups of center core. Chemical shift at 6.51 - 7.32 ppm indicate to aromatic protons. Triplet signal at 0.49 ppm refers to CH_2CH_3 protons, the, the chemical shift at 1.24 ppm refer to methyl group protons at OCH_2-**$\underline{CH_2}$**-CH_3, sextet signal at 2.07 ppm (q, 8H, **O-CO$\underline{CH_2}$-**CH_2-). The doublet signal at 8.32 ppm (d.d 8H pyrrole refer to alkenic protons atbeta position in pyrrole

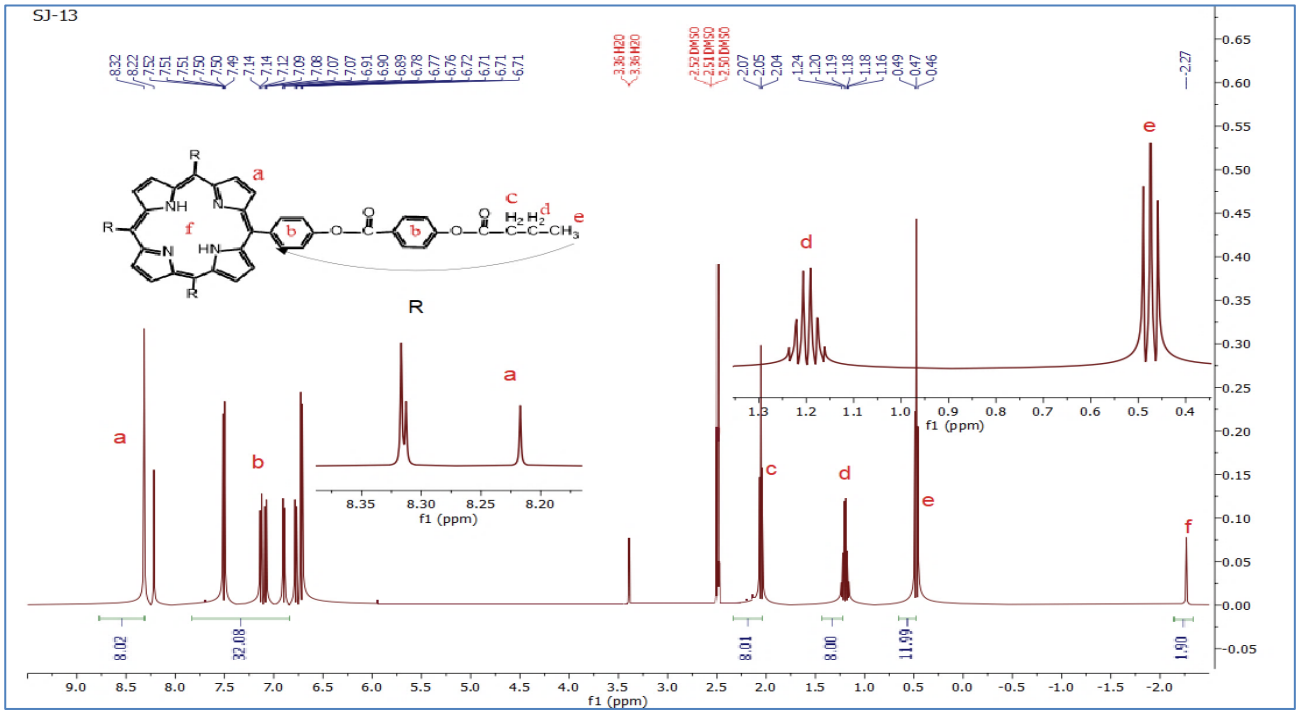

Fig. 9 ^{1}H-NMR spectrum of **S13** compound.

^{1}H-NMR spectrum of **S16** compound figure 10. Revealed the following: chemical shift at = - 2.36 ppm (s, 2H, NH) corresponding to the amine groups of center core. Chemical shift at 6.62- 7.43 ppm indicate to aromatic protons. Triplet signal at 0.31 ppm refers to methyl protons in (-CH_2CH_3) protons, the chemical shift at 2.03 ppm refers to methyl group protons at OCH_2CH_3, sextet signal at 1.06-0.66 ppm (m, 32H,CH_2CH_3), triplet signal at 1.96 ppm represent (**O-COCH$_2$CH$_2$**). The doublet signal at 8.23 ppm (d.d 8H pyrrole) refer to alkenic protons at beta position in pyrrole.

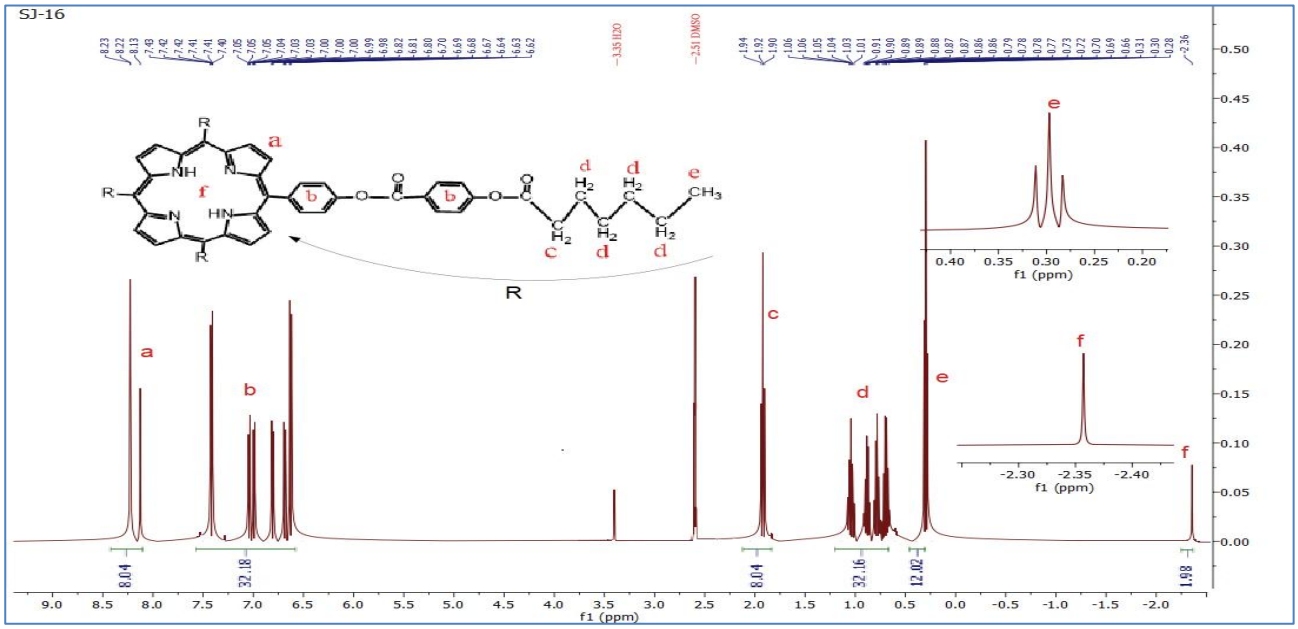

Fig. 10 ^{1}H-NMR spectrum of **S16** compound.

Table (3): Chemical Shift δ ppm of **(S11-S17).**

Comp. Symb.	Chemical Shift(ppm)	No. of Protons	Type of signal	Group
S11	-2.27	2	s	NH Pyrrole
	7.52-6.62	32	dd	Ar-H
	1.78	12	s	$-CH_3$
	8.32	8	dd	-C=CH Pyrrole
S12	-2.47	2	s	NH Pyrrole
	7.32-6.51	32	dd	Ar-H
	0.51	12	t	O-CO-CH_2-CH_3
	1.93	8	q	O-CO-CH_2-CH_3
	8.12	8	dd	-C=CH Pyrrole
S13	-2.27	2	s	NH Pyrrole
	7.52-6.71	32	dd	Ar-H
	0.49	12	t	CH_2-CH_3
	1.24	8	h	O-COCH_2-CH_2-CH_3)
	2.07	8	t	O-COCH_2-CH_2-
	8.32	8	dd	-C=CH Pyrrole
S14	-2.27	2	s	NH Pyrrole
	7.52-6.71	32	dd	Ar-H
	0.43	12	t	CH_2-CH_3
	1.02	8	h	CH_2-CH_2-CH_3
	1.36	8	p	-CH_2-CH_2-CH_2
	2.04	8	t	O-COCH_2-CH_2-
	8.32	8	dd	-C=CH Pyrrole
S15	-2.37	2	s	NH Pyrrole
	7.42-6.61	32	dd	Ar-H

	0.28	12	t	CH_2-CH_3
	0.78-0.68	16	m	CH_2CH_2-CH_2-CH_3
	1.17	8	p	O-$COCH_2CH_2$-CH_2
	1.96	8	t	O-$COCH_2CH_2$
	8.22	8	dd	-C=CH Pyrrole
S16	-2.36	8	s	NH Pyrrole
	7.43-6.62	32	dd	Ar-H
	0.31	8	t	CH_2-CH_3
	1.06-0.66	32	m	CH_2-$(CH_2)_4$-CH_3
	1.94	8	t	O-$COCH_2CH_2$-
	8.23	8	dd	-C=CH Pyrrole
S17	-2.37	2	s	NH Pyrrole
	7.42-6.61	32	dd	Ar-H
	0.30	12	t	CH_2-CH_3
	0.71-0.60	48	m	CH_2-$(CH_2)_6$-CH_3
	1.06	8	p	O-$COCH_2CH_2$-CH_2
	1.93	8	t	O-$COCH_2CH_2$-
	8.22	8	dd	NH Pyrrole

^{13}C-NMR spectrum of **S11** compound (Figure 11) showed the following data: the signal at δ= 174.98 ppm, attributed to C=O of the terminal carbonyl group in the ester, the signal at δ= 171. 14 ppm, attributed to C=O of the middle carbonyl group in the ester, the signal at δ= 162.39 ppm, attributed to C-O ester group in the middle, the signal at δ= 166.02 ppm, attributed to C-O ester group in the terminal, the signals at range δ= 131.79-120.92ppm, refer to aromatic carbons. The signal at δ= 156.16ppm corresponds to (C=N) group in pyrrole section, the signal at δ= 151.95 ppm refer to C-N in pyrrole rings, the signal at δ= 22.28 ppm, attributed to CH_3 group .

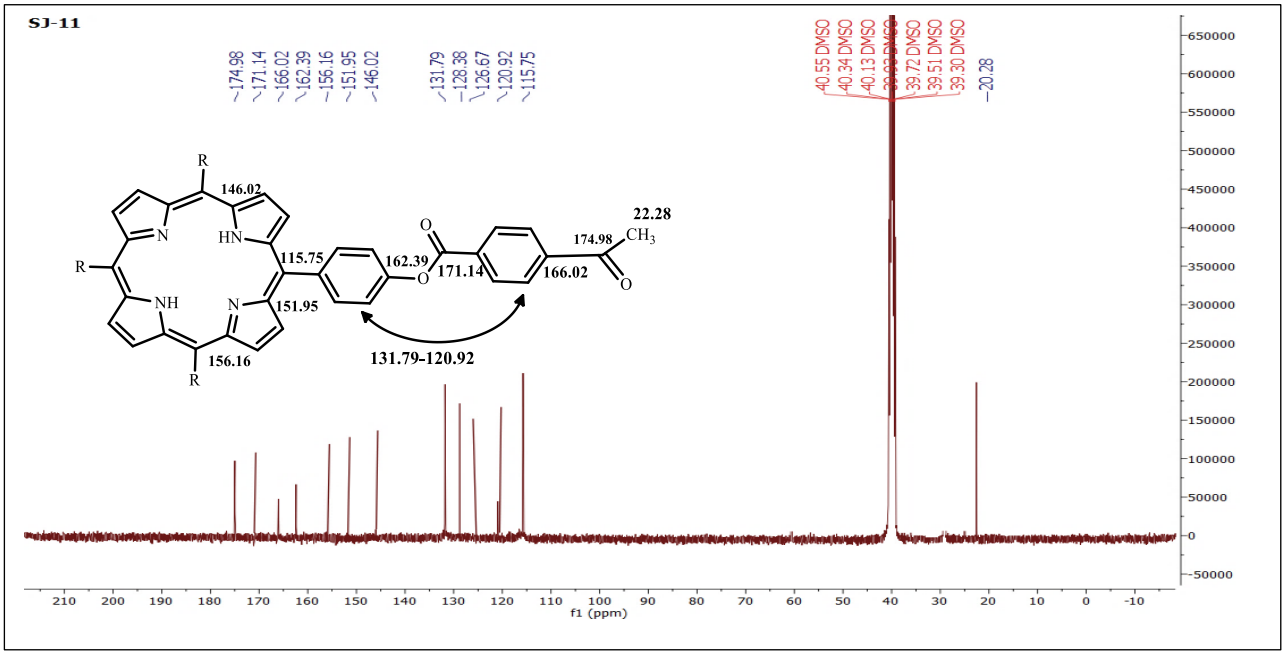

Fig. 11 ^{13}C-NMR spectrum of **S11** compound.

^{13}C-NMR spectrum of **S17** compound (Figure 12) showed the following data: the signal at δ= 174.98 ppm, attributed to C=O of the terminal carbonyl group in the ester, the signal at δ= 171. 14 ppm, attributed to C=O of the middle carbonyl group in the ester, the signal at δ= 162.39 ppm, attributed to C-O ester group in the middle, the signal at δ= 166.02 ppm, attributed to C-O ester group in the terminal, the signals at range δ= 131.79-120.92ppm, refer to aromatic carbons. The signal at δ= 156.16ppm corresponds to (C=N) group in pyrrole section, the signal at δ= 151.95 ppm refer to C-N in pyrrole rings, the signal at δ= 22.28 ppm, attributed to CH_3 group.

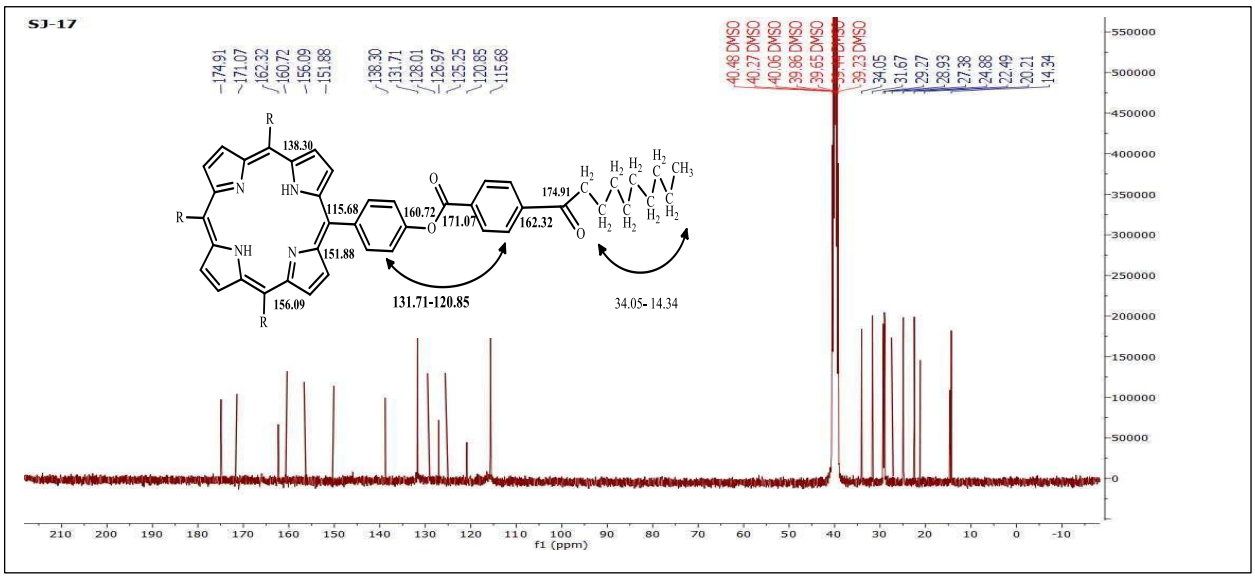

Fig. 12 ^{13}C-NMR spectrum of **S17** compound.

Estimation of liquid crystal behavior of synthesized compound:

The liquid crystal phases of new porphyrin esters (S11-17) were studied and characterized by polarized light microscope equipped with a heater (POM) by a small amount of substance (0.05 – 0.1)g where by heating the sample in (POM) device with thermal rate (5-10) m\min. [24], [25]Shown in Figures 13 for compounds S12, S13,S14 and S15 respectively.

Table 4: liquid crystal properties of synthesized compounds.

Comp.	POM	Heat	Cr %	S-Col_h	S-Col_r	ND	ΔS Col_h	ΔS Col_r	ΔND
S11	POM	Heat	275						
S12	POM	Heat	273			297			24
S13	POM	Heat	268			286			18
S14	POM	Heat	264			279			15
S15	POM	Heat	261	275		287	14		12
S16	POM	Heat	270						
S17	POM	Heat	279						

Cr=Crystal phase.
S-Col_h= smectic column hexogonal phase. ,S-Col_r= smectic column rectengolar phase.
ND= nematic discotic phase.

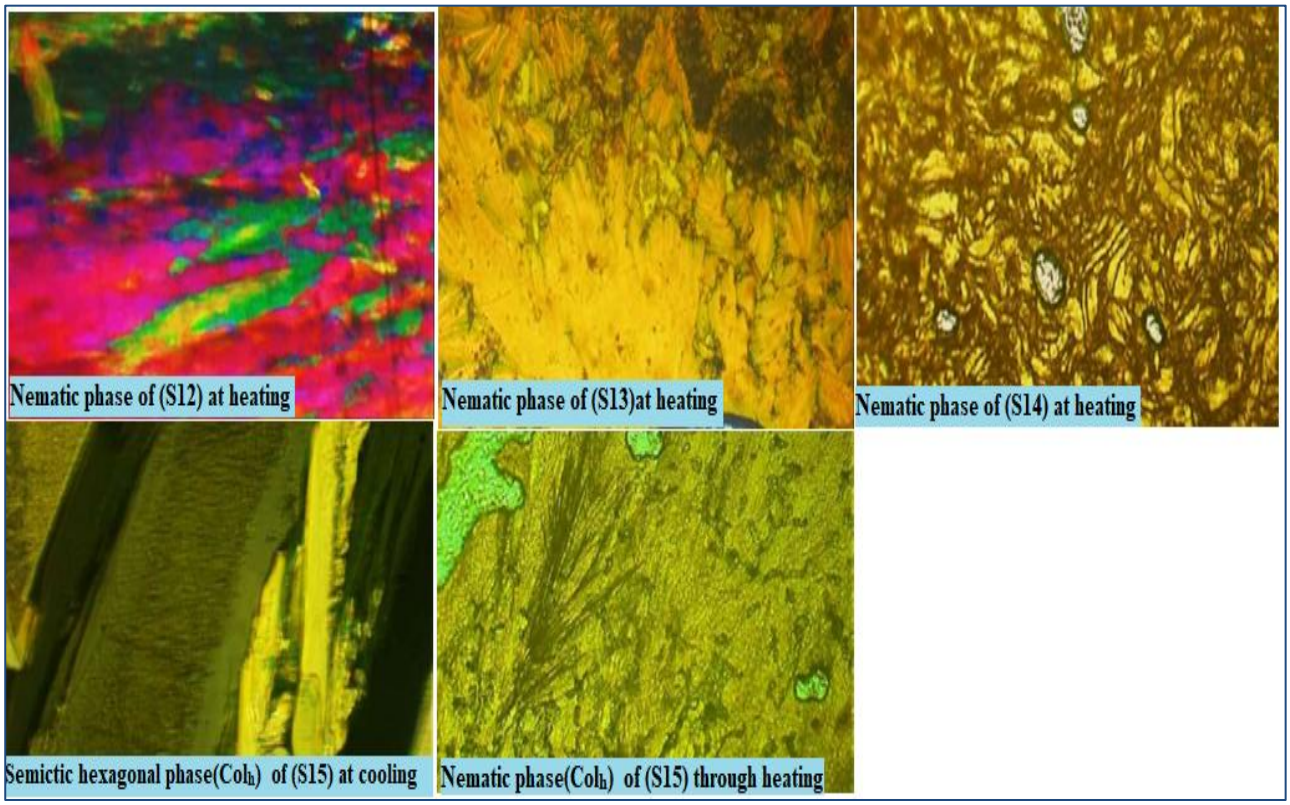

Fig. 13 liquid crystal texture of synthesized compounds.

The organic compounds to be studied contain one ester linked group as well as aliphatic terminal group.

From outcomes for this compound that listed in table (4): almost tested certain compound of this series showed liquid crystal phases with thermal transition according to the nature of compound, the causes of this behavior attributed to the compound designated by scenario discotic form, with high regularity because the molecule contain four bounded core with aromatic ring that elevate hardness of molecule.

In addition, it was observed that the thermal stability of the nematic phase increases as the length of the aliphatic chains decreases, and the reason for this is the decrease in the end-bonding force with increasing the length of the aliphatic chain, as this force favors the emergence and stability of the nematic phase. On the contrary, increasing the length of the aliphatic chains increases the thermal stability of the identified smectic phases. It was observed that all compounds of this series have high transition degrees, and the reason for this is due to the molecules having high molecular weights, in addition to the presence of highly electronegative nitrogen atoms in the core of the molecule, which increases the bonding force between the molecules by forming two types of forces: dipole-dipole or formation[26], [27]

The results that observed showed all compounds of this series have high degrees of transition, and the reason for this is due to the fact that the molecules have high molecular weights, in addition to the presence of nitrogen atoms with high electronegativity in the core

of the molecule, which increases the strength of the bond between the molecules by forming two types of forces, dipole-dipole or forming hydrogen bonds, and thus increasing the temperatures at which the transition occurs also the additional ester group linked to aromatic rings has been inserted into the structure of the molecule, that elevate the rigidity of this designated compounds[28],[29]

The results of the polarized light microscope (POM) test of the compounds of this series, as shown in Table (4), that part of the compounds of this series did not show liquid crystalline phases. The reason for this is perhaps due to the increase in the hardness of the molecule by introducing additional aromatic systems in the middle of the molecule, in addition to the presence of unpaired electron pairs of the added ester oxygen atom, which leads to the loss of part of the equatorially of the compound therefore loss of the liquid crystalline character.

The final conclusion of the study of the liquid crystalline property of the compounds of these two series is that all the compounds that showed the liquid crystalline property were only in heating, i.e. the compounds were of the monotropic liquid crystal type[30],[31].

In addition to that remember above the thermal stability of nematic discotic phase observed increase with the length of aliphatic chain.

Antibacterial activity:

On the other hand, the research program included estimation the effectiveness of these novel porphyrin derivatives as an antibacterial agent against types of bacteria with common pathogenic infections. This types are *Escherichia coli* and *Staphylococcus aureus,* the obtained results indicates that the S11, S12 and S13 showed reasonable activity[32] as presented in the table 5 and figure14,15 respectively.

Table (5): outcomes of antibacterial potency of porphrin derivatives**(S11-S17)**.

compound	Zone of inhibition (mm)							
	E.coli				S.aureus			
Concentration(g/ ml)	5	10	15	20	5	10	15	20
S11	0	0	8	11	0	0	0	10
S12	0	0	9	13	0	0	7	9
S13	0	0	7	11	0	0	0	10
S14	0	0	0	0	0	0	0	0
S15	0	0	0	0	0	0	0	0
S16	0	0	0	0	0	0	0	0
S17	0	0	0	0	0	0	0	0
Amikasin	13	19	23	25	5	11	16	19

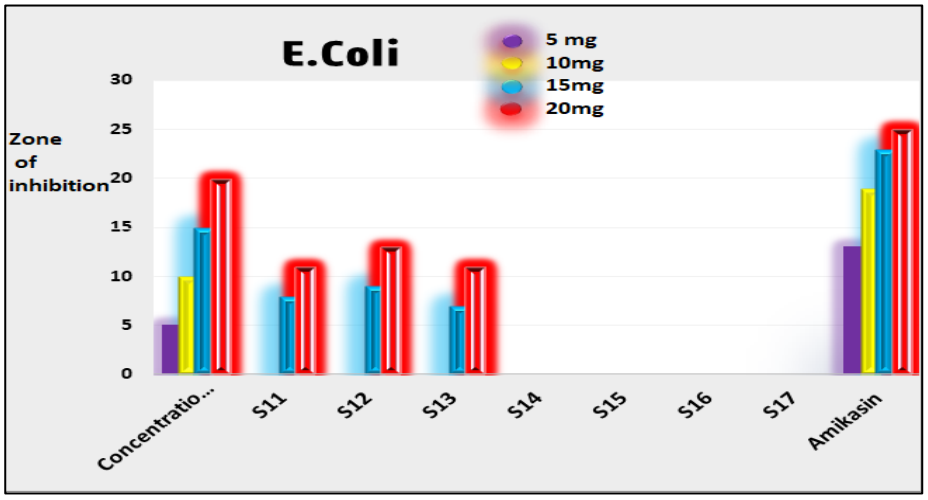

Fig. 14 represented data of porphyrin derivatives against E.Coli**.**

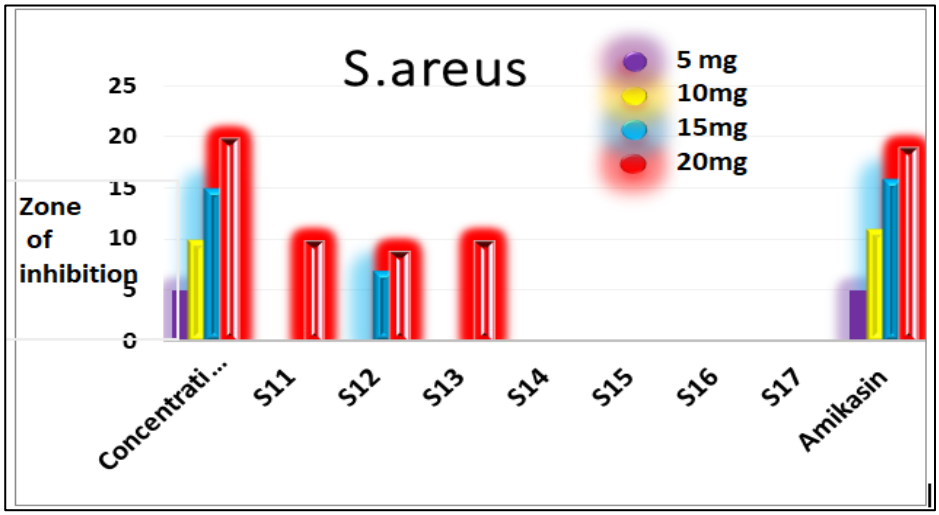

Fig. 15 represented data of porphyrin derivatives against S.areus.

3.7. Molecular docking:

In this part molecular docking was performed for the compounds (**S11**) against of biotin carboxylase (PDB:ID:**3jzf**) in E. coli pathogenic bacteria and biotin protein ligase (PDB:ID**:4dq2**) in S.arues pathogenic bacteria, the results of simulation as follow:

Molecular docking results that obtained in this section indicated that the compounds (**S11**), figure 16. interacted with biotin carboxylase (PDB:ID:**3jzf**) in E.coli at a good values regarding of docking score , RMSD, hydrogen bonds, docking score =-8.7 kcal\mol, RMSD value (2.989 A^{o}) , 2D and 3D screened visualized picture showed presence five hydrogen bonds: (B:SER56with carbonyl group), (B:PHE84with carbonyl group), S11 compound, figure 17, also interacted with biotin protein ligase (PDB:ID**:4dq2**) in S.arues at docking score =-8.5 kcal\mol, RMSD value (1.757 A^{o}) , 2D and 3D screened visualized picture showed presence five hydrogen bonds: (A:GLN28 with carbonyl group), A:GLN52 with oxygen), (A:ARG250 with **C=O** group as well as pi-anion,pi-cation…etc interaction[20].As shown in the following table (6).

Table (6): Outcomes of Molecular docking for antibacterial active compounds.

S11	PDB:ID	Docking score (kCal/mol)	RMSD l.b. (A°)	RMSD u.b. (A°)	Type of H.bond
S11	3jzf	-8.7	2.989	5.444	B:SER56 B:SER56 B:PHE84
S11	4dq2	-8.5	1.757	3.663	A:GLN28 A:GLN52 A:ARG250
S12	4dq2	-8.9	2.255	3.88	A:GLN28 A:GLN52 A:ARG250

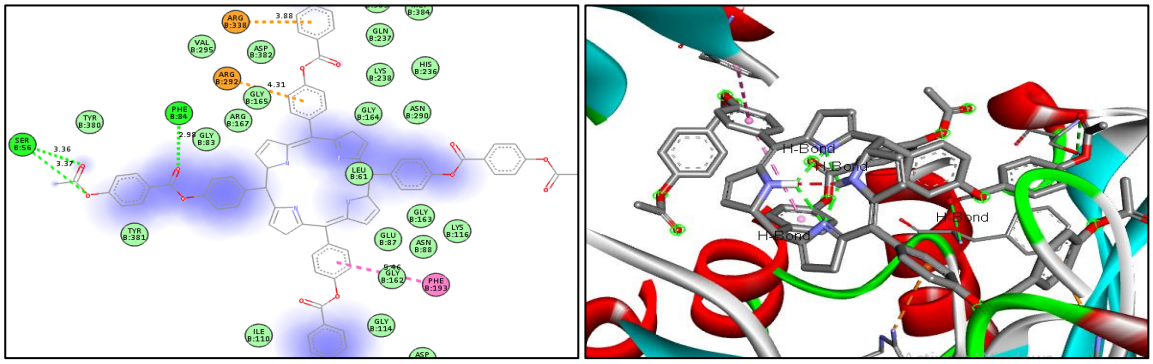

Figure. 16 Molecular docking visualization 2D (left) and 3D (right) of S11 derivatives with biotin carboxylase (PDB:ID:3jzf) in E. coli.

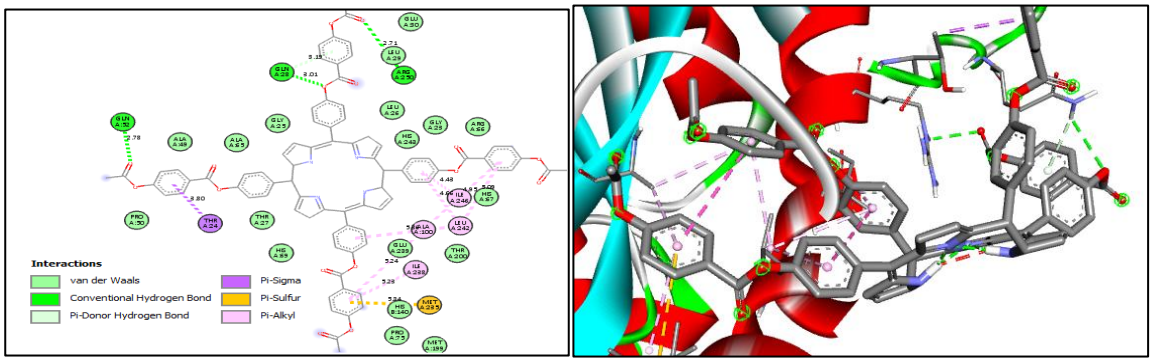

Figure. 17 Molecular docking visualization 2D (left) and 3D (right) of S11 derivatives against biotin protein ligase (PDB:ID:4dq2)S.areus.

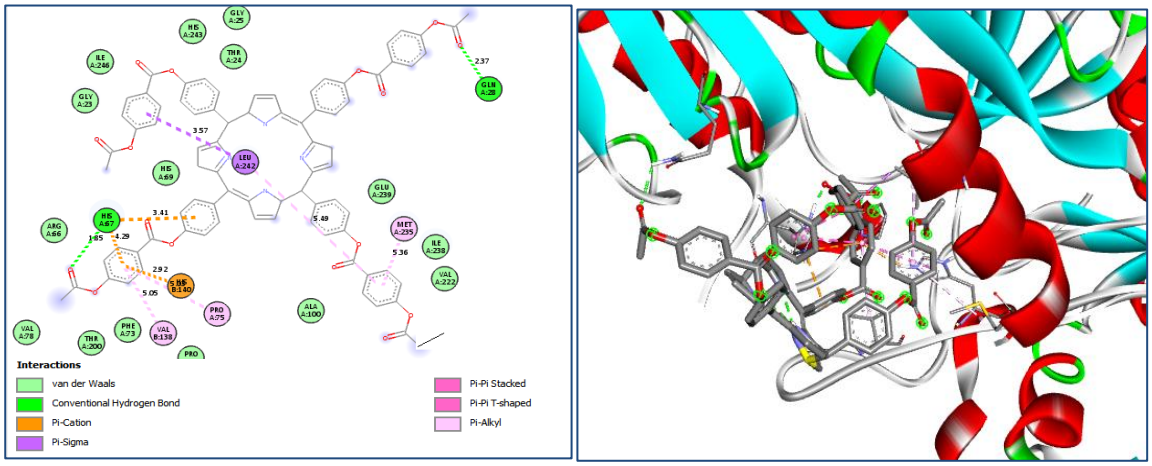

Figure. 18 Molecular docking visualization 2D (left) and 3D (right) of S12 derivatives against biotin protein ligase (PDB:ID:4dq2)S.areus.

Conclusions

The synthesized compounds **S11-S17** were prepared with good yield, the synthetic pathway revealed the possibility of modifying porphyrin into the derivatives that distinctive advantageous, the new porphyrin showed a good liquid crystal properties with several liquid phases such as discotic and nematic, the results of, the short flexible tail have reasonable anti-bacterial behavior molecular docking showed the derivatives interacted with a good docking score and best binding images.

Acknowledgment:

The authors present the great thankful for the Depart of Chemistry, College of Science, University of Tikrit.

References:

[1] M. S. Thakur *et al.*, "Metal coordinated macrocyclic complexes in different chemical transformations," *Coord. Chem. Rev.*, vol. 471, p. 214739, 2022.

[2] T. D. Lash, "Coordination chemistry of modified porphyrinoid systems," *Chem. Rev.*, vol. 122, no. 9, pp. 7987–7989, 2022.

[3] K. Watanabe, N. N. Pati, and Y. Inokuma, "Contracted porphyrins and calixpyrroles: synthetic challenges and ring-contraction effects," *Chem. Sci.*, vol. 15, no. 19, pp. 6994–7009, 2024.

[4] M. Stepien, E. Gonka, M. Żyła, and N. Sprutta, "Heterocyclic nanographenes and other polycyclic heteroaromatic compounds: synthetic routes, properties, and applications," *Chem. Rev.*, vol. 117, no. 4, pp. 3479–3716, 2017.

[5] W.-L. Chan, C. Xie, W.-S. Lo, J.-C. G. Bünzli, W.-K. Wong, and K.-L. Wong, "Lanthanide–tetrapyrrole complexes: synthesis, redox chemistry, photophysical properties, and photonic applications," *Chem. Soc. Rev.*, vol. 50, no. 21, pp. 12189–12257, 2021.

[6] S. Thunell, "Porphyrins, porphyrin metabolism and porphyrias. I. Update," *Scand. J. Clin. Lab. Invest.*, vol. 60, no. 7, pp. 509–540, 2000.

[7] P. J. Brothers and M. O. Senge, “An Introduction to Porphyrins for the Twenty-First Century,” *Fundam. Porphyr. Chem. A 21st Century Approach*, vol. 1, pp. 1–8, 2022.

[8] F. A. da Silva Figueira, “Expanded Porphyrins and Their Evaluation as Anion Chemosensors,” 2016, *Universidade de Aveiro (Portugal)*.

[9] A. A. Fadda, R. E. El-Mekawy, A. El-Shafei, H. S. Freeman, D. Hinks, and M. El-Fedawy, “Design, synthesis, and pharmacological screening of novel porphyrin derivatives,” *J. Chem.*, vol. 2013, no. 1, p. 340230, 2013.

[10] Z. Wang *et al.*, “Recent advances in porphyrin-based MOFs for cancer therapy and diagnosis therapy,” *Coord. Chem. Rev.*, vol. 439, p. 213945, 2021.

[11] V. Nankivell *et al.*, “Biomimetic porphyrin-lipid nanoparticles-novel nanoscale theranostics for multimodal imaging and therapy in atherosclerotic cardiovascular disease,” *Eur. Heart J.*, vol. 45, no. Supplement_1, pp. ehae666-3874, 2024.

[12] G. D. Bajju, S. Kundan, M. Bhagat, D. Gupta, A. Kapahi, and G. Devi, “Synthesis and spectroscopic and biological activities of Zn (II) porphyrin with oxygen donors,” *Bioinorg. Chem. Appl.*, vol. 2014, no. 1, p. 782762, 2014.

[13] A. Sułek, B. Pucelik, M. Kobielusz, A. Barzowska, and J. M. Dąbrowski, “Photodynamic inactivation of bacteria with porphyrin derivatives: effect of charge, lipophilicity, ROS generation, and cellular uptake on their biological activity in vitro,” *Int. J. Mol. Sci.*, vol. 21, no. 22, p. 8716, 2020.

[14] H. Tasli, A. Akbiyik, V. Alptuzun, and S. Parlar, “Antibacterial activity of porphyrin derivatives against multidrug-resistant bacteria.,” *Pak. J. Pharm. Sci.*, vol. 32, no. SI5, pp. 2369–2374, 2019.

[15] A. Vega-Medina, S. Pérez-Gutiérrez, J. Pérez-Ramos, C. Martínez-Nava, and C. Pérez-González, “Synthesis and pharmacological evaluation of free-base 5, 10, 15, 20-tetrakis (4-hydroxyphenyl) porphyrin and its Zn, Cu, Co metalloderivatives,” 2022.

[16] H. A. Idham, H. K. Salih, and I. K. Jassim, “Synthesis, Characterization and Computational Study of Discotic Liquid Crystal Compounds,” 2021.

[17] D. A. Ibrahim and H. K. Salih, “SYNTHESIS, CHARACTERIZATION, AND STUDY OF THE CRYSTALLINE PROPERTIES OF ASTERISM COMPOUNDS,” *Kim. Probl.*, vol. 22, no. 4, pp. 478–488, 2024.

[18] A. H. Kshash, O. J. M. Al-Asaf, and H. K. Salih, “Synthesis, Characterization, and Investigation of Mesomorphic Properties of a New 2, 5-Bis-(4-alkanoyloxybenzylidene) cyclopentan-1-one,” 2022.

[19] S. T. Sadiq, “Investigation of Class 1 Integrons (intl1) and Insertion Sequences Common Region (ISCR1) Genes Cassette in Multidrug Resistance Bacteria,” *Environments*, vol. 2, p. 4, 2025.

[20] Z. A. Dawood, F. D. Khalid, and A. S. Hameed, "Synthesis, radical scavenging activity, antibacterial activity and molecular docking of a new thiazolidine-4-one and 1, 3, 4 oxadiazole derivatives of tolfenamic acid," *Synthesis (Stuttg).*, vol. 45, no. 02, 2022.

[21] M. Aydin, "DFT and Raman spectroscopy of porphyrin derivatives: Tetraphenylporphine (TPP)," *Vib. Spectrosc.*, vol. 68, pp. 141–152, 2013.

[22] W. Liu *et al.*, "Synthesis and characterization of liquid crystalline 5, 10, 15, 20-tetrakis (4-n-alkanoyloxyphenyl) porphyrins," *Liq. Cryst.*, vol. 30, no. 11, pp. 1255–1257, 2003.

[23] K. Vosmann, B. Wiege, P. Weitkamp, and N. Weber, "Preparation of lipophilic alkyl (hydroxy) benzoates by solvent-free lipase-catalyzed esterification and transesterification," *Appl. Microbiol. Biotechnol.*, vol. 80, pp. 29–36, 2008.

[24] R. H. Saleh, W. M. Rashid, A. H. Dalaf, K. A. Al-Badrany, and O. A. Mohammed, "Synthesis of some new thiazolidinone compounds derived from schiff bases compounds and evaluation of their laser and biological efficacy," *Ann Trop Public Heal.*, vol. 23, no. 7, pp. 1012–1031, 2020.

[25] I. A. Yass, M. M. Aftan, A. H. Dalaf, and F. H. Jumaa, "Synthesis and identification of new derivatives of bis-1, 3-oxazepene and 1, 3-diazepine and assess the biological and laser efficacy for them," in *The Second International & The Fourth Scientific Conference of College of Science–Tikrit University. P*, 2020, pp. 77–87.

[26] K. Ruan, X. Zhong, X. Shi, J. Dang, and J. Gu, "Liquid crystal epoxy resins with high intrinsic thermal conductivities and their composites: A mini-review," *Mater. Today Phys.*, vol. 20, p. 100456, 2021.

[27] P. Lv *et al.*, "Stimulus-driven liquid metal and liquid crystal network actuators for programmable soft robotics," *Mater. Horizons*, vol. 8, no. 9, pp. 2475–2484, 2021.

[28] Y.-L. Li *et al.*, "Tunable liquid crystal grating based holographic 3D display system with wide viewing angle and large size," *Light Sci. Appl.*, vol. 11, no. 1, p. 188, 2022.

[29] I. Kim *et al.*, "Stimuli-responsive dynamic metaholographic displays with designer liquid crystal modulators," *Adv. Mater.*, vol. 32, no. 50, p. 2004664, 2020.

[30] J. Uchida, B. Soberats, M. Gupta, and T. Kato, "Advanced functional liquid crystals," *Adv. Mater.*, vol. 34, no. 23, p. 2109063, 2022.

[31] K. Yin *et al.*, "Advanced liquid crystal devices for augmented reality and virtual reality displays: principles and applications," *Light Sci. Appl.*, vol. 11, no. 1, p. 161, 2022.

[32] F. D. Gonelimali *et al.*, "Antimicrobial properties and mechanism of action of some plant extracts against food pathogens and spoilage microorganisms," *Front. Microbiol.*, vol. 9, p. 1639, 2018.

IRAQI Academic Scientific Journals
Samarra Journal of Pure and Applied Science
SJPAS
مجلة سامراء للعلوم البحتة والتطبيقية
www.sjpas.com
p ISSN: 2663-7405
e ISSN: 2789-6838

تحضير، تشخيص، دراسة الخصائص البلورية السائلة، محاكاة الارساء الجزيئي والفعالية ضد البكتيريا لاسترات جديدة مشتقة من البورفرين

ستار جبير معيوف ، هناء كائن صالح
قسم الكيمياء، كلية العلوم، جامعة تكريت، العراق

معلومات البحث:
تاريخ الاستلام: 2025/02/10
تاريخ التعديل: 2025/03/10
تاريخ القبــول: 2025/03/15
تاريخ الـنشر: 2025/12/30
الكلمات المفتاحية:
بلورات سائلة، ارساء جزيئي، استرت البورفرين، فعالية ضد البكتريا.

معلومات المؤلف
الايميل:
الموبايل:

الخلاصة:

تضمن هذا البحث تحضير استرات جديدة مشتقة من البورفرين حيث حضرت نواة البورفرين من تفاعل البايرول مع بارا-هيدروكسي بنزالديهايد بوجود حامض البروبانويك، تم ربط مركب بارا-هيدروكسي اثيل بنزوات S9 مع نواة البورفرين للحصول على المشتق S10 تمت استرة المشتق S10 مع كلوريدات حوامض كاربوكسيلية مختلفة للحصول على مشتقات S11-S17 ان التركيب الكيميائي للمركبات النهائية تم اثباته بواسطة: FT-IR و ^{1}H-NMR و ^{13}C-NMR حيث اثبتت النتائج المستحصلة صحة التراكيب المقترحة فيما درست الخصائص البلورية السائلة لهذه المركبات بواسطة المقطاب الضوئي مع الحرارة (POM) حيث اظهرت المشتقات S14S12,S13,S15 خصائص واطوار بلورية مميزة، تمت دراسة الارساء الجزيئي للمشتقات S11,S12,S13 حيث اظهرت النتائج درجات ارتباط وصور ارتباط جيدة.